flow of conversion products $G_{c.p}$. To increase the latter the diameter of the circulating corundum particles was chosen equal to 0.5 mm. The mathematical model allowed using the temperature and methane concentration distributions within the reactor (Fig. 3, curve 7) to obtain the required height of the catalytic packing (H = 1 m).

The construction of the reactor designed is shown in Fig. 4, while its basic operating parameters are presented in Table 3. After construction designs were developed, the reactor was converted from operation with water vapor to use for conversion of methane gas when fed by the circulation gas exiting from a furnace used for reduction fo iron ore nodules (composition: CH_4, 3.0; CO, 20.1; CO_2, 17.2; H_2, 42.0; H_2O, 14.2; N_2, 3.5%). Such reactors can be used to replace low reliability tube furnaces which require large expenditures of imported high alloy steel and catalyst.

NOTATION

c, mean mass specific heat at constant pressure per 1 kg methane supplied to the reactor, J/(kg·K); d, particle diameter, mm; E, activation energy, J/mol; G, mass flow rate, kg/(m²·sec); H, catalytic packing height, m; k, chemical reaction rate constant, m/sec; m, quantity of methane required for production of 1 kg of conversion product, kg; P, pressure, atm; q_{c1}, q_{c2}, heats of chemical reactions (1) and (2), J/kg of natural gas; q_3, q_5, heat losses for incomplete combustion and to surroundings; q, heat, J/kg of natural gas; R, universal gas constant, J/(mol·K); r, volume content of methane; s, specific surface of catalytic packing, m^2/m^3; t, temperature, °C; W, fluidization number; x, fraction of conversion product removed from reactor; z, vertical coordinate, m (measured from lower face of catalytic packing toward upper); ρ, density, kg/m^3; ε, packing porosity; λ, effective heat transfer coefficient, W/(m·K). Subscripts: a, air; o, original; f, final; m, methane; n.c, normal conditions; v, vapor; c.p, conversion products; com, combustion products.

LITERATURE CITED

1. A. M. Dubinin, A. P. Baskakov, and V. B. Shoibonov, Inventor's Certificate No. 992079, "Endothermal atmosphere generator," Byull. Izobret., No. 4 (1983).
2. A. P. Baskakov, B. V. Berg, A. F. Ryzhkov, and N. F. Filippovskii, Heat and Mass Transport Processes in a Fluidized Bed [in Russian], Moscow (1978).

STRIKING DYNAMICS AND ENERGY CHARACTERISTICS OF A BULK DISCHARGE WITH UV PREIONIZATION NEAR THE THRESHOLD VOLTAGE

V. N. Karnyushin, P. P. Samtsov, and R. I. Soloukhin

UDC 621.375

Measurements have been made on the effects of preionization on the striking and energy characteristics of a bulk discharge near the threshold voltage.

Considerable use is made of UV preionization in pulsed laser systems, which has stimulated numerous studies on the ionization and energy characteristics [1-3]. A necessary condition for obtaining a bulk discharge (BD) at pressures of about 1 atm is the production of an initial electron density n_0 of about 10^6-10^8 cm^{-3} in the gap, while the electrodes subsequently receive a voltage pulse whose amplitude U_0 exceeds some threshold value U_1 slightly dependent on n_0 [4, 5].

There is interest in the striking dynamics and energy characteristics of BD for U_0 close to U_1 primarily because then the ratio of the electric field E to the gas pressure P lies closest to the value optimal for pumping CO_2 laser levels [2]. The highest efficiency is

Lykov Institute of Heat and Mass Transfer, Academy of Sciences of the Belorussian SSR, Minsk.

Translated from Inzhenerno-Fizicheskii Zhurnal, Vol. 52, No. 1, pp. 86-89, January, 1987. Original article submitted September 17, 1985.

0022-0841/87/5201-0068$12.50

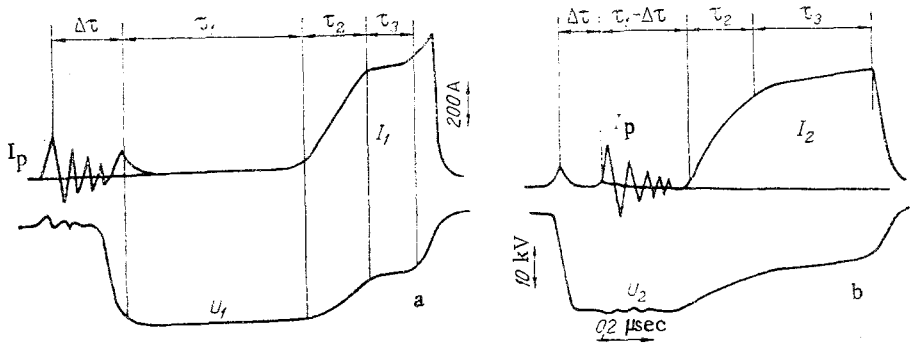

Fig. 1. Waveforms for the current I and voltage U in the main discharge and for the preionization current I_p: a) preionizer switched in advance of voltage pulse on discharge gap; b) with delay.

attained in a pulsed CO_2 laser with UV preionization for $U_0 = U_1$ [6]. At the same time, the discharge build-up time increases when the voltage is near threshold, which enables one to distinguish the major phases [7] and to elucidate the initiation and striking in dense gases.

We have examined a bulk discharge with UV preionization at voltages near threshold and have determined the optimum striking conditions.

We used a typical system for producing a BD with independent preionizer switching. The gap volume for the main discharge was 1.5 × 2.4 × 10 cm, gap between the electrodes d = 1.5 cm. The preionization was provided by a sectional discharge over the surface of an insulator involving parallel switching of gaps distributed uniformly in the plane with a density of about 1 cm^{-2}. The preionizer lay behind the grid anode at 0.6 cm from the main discharge zone. The preionizer discharge was supplied from a low-inductance capacitor of 0.1 μF charged to 3-13 kV. Resistance-capacitance voltage decay substantially complicates examining the dynamic characteristic, so the main discharge was supplied from a cable line having a surge impedance of 25 Ω, which was connected to the gap via a controlled discharge gap and provided square pulses of duration 10^{-6} sec. The mixture was CO_2:N_2:He = 1:1:4 at atmospheric pressure.

The current and voltage waveforms were recorded for the main and auxiliary discharges.

Figure 1 shows that the preionization current has damped oscillations, damping time about 0.2 μsec. The charging voltage for the main discharge (U_0 = 24 kV) was equal to the static breakdown voltage U*. Three discharge stages can be seen: 1) ionization develops in the discharge gap over a time τ_1, this being characterized by a low current, hardly seen on the waveforms, 2) breakdown completion, during which there is a rapid rise in the current density to about 10 A/cm^2 in about 0.1 μsec, and 3) quasistationary burning of the bulk glow discharge, which is characterized by slow increase in the current density evidently on account of gas heating, together with the transition over a time τ_3 to a spark discharge (the start of the transition is recorded in Fig. 1a).

These waveforms show that the initiation mode has an appreciable effect on τ_1 and τ_3, as well as on the limiting energy deposition in the BD.

Figure 2 shows how τ_1 is dependent on the interval $\Delta\tau$ between supplying the voltage to the discharge gap and switching the preionizer. There is a certain range in $\Delta\tau$ providing the minimum τ_1 for given initial voltages on the main and auxiliary discharges. Also, if the preionizer is switched with a delay ($\Delta\tau > 0$), the figure gives the interval $\tau_1 - \Delta\tau$ corresponding to ionization growth with the auxiliary discharge switched on; $\tau_1 - \Delta\tau$ decreases as $\Delta\tau$ increases.

We consider the processes occurring in the discharge gap as the ionization grows. When the voltage is applied to the gap, avalanche multiplication starts for the electrons of initial concentration n_0, which is determined by the natural background (for $\Delta\tau > 0$) or by the preionization source (for $\Delta\tau < 0$). The criterion of [4] for diffusion overlap between avalanches, which defines the minimal initial electron concentration, becomes irrelevant for voltages $U_0 \leq U^*$ insufficient for a single avalanche to become a streamer. The length of the primary-avalanche generation stage for an electron drift velocity $v \approx 10^7$ cm/sec is d/v = 01.5 μsec, which is much less than the measured minimal τ_1, while the maximal current density j_m defined by $j_m = evn \leq \alpha vE/4\pi$ from the condition for a space-charge restriction on the ionization rate

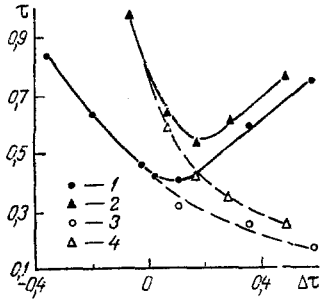

Fig. 2

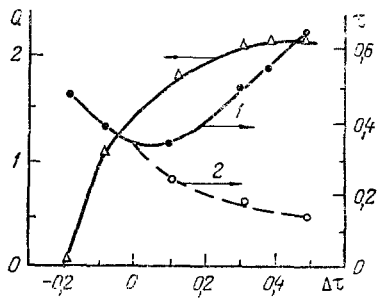

Fig. 3

Fig. 2. The $\Delta\tau$ dependence of the ionization rise time τ_1 (1 and 2) and $\tau_1 - \Delta\tau$ (3 and 4) for U_0 = 24 kV: 1 and 3) charging voltage 11 kV; 2 and 4) charging voltage 9 kV; τ and $\Delta\tau$ in μsec.

Fig. 3. The $\Delta\tau$ dependence of the limiting energy deposition Q and τ_1 (1) and $\tau_1 - \Delta\tau$ (2) for U_0 = 26 kV, charging voltage 3 kV; Q in J.

was about 0.1 A/cm^2 ($n_e \approx 6 \cdot 10^{10}$ cm^{-3}) under these conditions, which is substantially less than the values of the waveforms. This means that much of τ_1 is taken up by ionization involving the generation of secondary avalanches, whose intensity is determined to a considerable extent by the electron reproduction rate in the cathode region arising from radiation emitted by the highly ionized anode layer.

Delayed preionizer switching evidently intensifies the production of secondary avalanches during the striking; an important point is that the electric field is strengthened by the ion space charge [8]. The number of ionizations produced by an electron in the distorted electric field exceeds the number of ionizations in the field $E_0 = U_0/d$ if $E_0 = E^* < BP/2$, where B is the constant appearing in the semiempirical relation for the Townsend ionization coefficient $\alpha/P = A \exp(-BP/E)$. The significance of this factor increases with $\Delta\tau$, so the discharge build-up time $\tau_1 - \Delta\tau$ decreases (Fig. 2).

Delayed preionizer switching increases the stability margin and the limiting energy deposition. Figure 3 shows that the maximum deposition corresponds to minimal $\tau_1 - \Delta\tau$ when $\Delta\tau > 0$. The experiments show that this preionizer switching mode is optimal for charging voltages $U_0 \leq 1.25\ U^*$.

NOTATION

n_0, electron density; U_0, initial voltage on the main discharge electrode; U_1, lower limit to main discharge striking; U_a, voltage on additional discharge condenser; U^*, static breakdown voltage; U, discharge burning voltage; I, discharge current, τ_1, ionization rise time in discharge gap; τ_2, breakdown completion time; τ_3, quasistationary discharge burning time; $\Delta\tau$, time between applying voltage to discharge gap and switching on preionizer; e, electron charge; v, electron drift velocity; α, Townsend collision ionization coefficient; A, B, constants in semiempirical relation for α; Q, energy deposition in bulk discharge.

LITERATURE CITED

1. V. N. Karnyushin and R. I. Soloukhin, Macroscopic and Molecular Processes in Gas Lasers [in Russian], Moscow (1981).
2. E. P. Velikhov, V. Yu. Baranov, V. S. Letokhov, et al., Pulsed CO_2 Lasers and Applications in Isotope Separation [in Russian], Moscow (1983).
3. G. A. Mesyats and D. I. Proskurovskii, A Pulsed Electric Discharge in Vacuum [in Russian], Novosibirsk (1984).
4. V. N. Karnyushin, A. N. Malov, and R. I. Soloukhin, Kvantovaya Elektron., 5, No. 3, 555-562 (1978).
5. H. Gündel, Beiträge aus der Plasmaphysik, 21, 393-402 (1981).
6. A. A. Kuchinskii, V. A. Rodichkin, and V. A. Smirnov, Zh. Tekh. Fiz., 50, 2567-2571 (1980).
7. V. N. Karnushin and P. P. Santsov, Proc. 15th ICPIG, Contrib. Paper, Minsk (1981), p. 853.
8. A. Engel and M. Steenbeck, The Physics and Engineering of Discharges in Gases [Russian translation], Moscow–Leningrad (1935).